

Electrochemical Characterisation of Nanocrystalline Nickel

Deepika Sachdeva, Naveen Gupta, and R. Balasubramaniam

Indian Institute of Technology, Kanpur-208 016

ABSTRACT

Nanocrystalline nickel (nc-Ni) coatings were produced by pulse electrodeposition using Watts bath with sodium citrate and saccharin added as grain refining agents. The electrochemical nature of nc-Ni coatings, evaluated in 1M H_2SO_4 solution by electrochemical impedance spectroscopy. The corrosion rate of bulk nickel was lower than that of nc-Ni after stabilisation of free corrosion potential.

Keywords: Nickel, electroplating, corrosion, electrochemical impedance spectroscopy, nanocrystalline nickel

1. INTRODUCTION

Nanocrystalline materials are being actively studied because of their unique combination of properties and their possible applications in several areas of modern technology. Electrodeposition is one of the most commercially applicable techniques for synthesis of nanocrystalline metals and alloys. Pulse electrodeposition allows high deposition current densities in contrast to the direct current deposition route¹. This is possible due to the replenishment of electrolyte at the electrolyte-substrate interface replenishment during the off time periods², thus allowing current densities even higher than the limiting current density. This establishes conditions of large overpotential and low surface diffusion rates, which are typically associated with higher nucleation rates and suppressed grain growth rates¹. Grain sizes of nano-scale can therefore be obtained with increased nucleation rates in pulse electrodeposition. Therefore, pulse electrodeposition route was chosen for the synthesis of nanocrystalline nickel (nc-Ni) in the present study.

Pulse electrodeposited nc-Ni can serve as corrosion and wear resistant coating³. The corrosion properties of nc-Ni have also been investigated^{4,5}. Rofagha⁴, *et al.* investigated the corrosion behaviour of nc-Ni (99.99 % purity, 32 nm grain size) and coarse grained nickel (99.99 %, 100 μ m grain size) in 1M H_2SO_4 . They found that the corrosion potential of nc-Ni was more noble compared to that of polycrystalline nickel. Mishra & Balasubramaniam⁵ have confirmed these results for nc-Ni. The passive current densities, determined from potentiodynamic polarization curves, of nc-Ni were higher than that of pure bulk Ni^{4,5}. Interestingly, the corrosion rate of nc-Ni decreased with decreasing grain size based on polarisation experiments conducted immediately on immersion⁵. This was related to a more uniform distribution of sulphur by pulse electrodeposition method, as has been found for nc-Co. Zeiger⁷, *et al.* reported enhanced corrosion resistance of nc-Fe-8 per cent Al in Na_2SO_4 solution (pH=6), which was attributed to protective oxide film formation due to fast diffusion of Al through the grain boundaries.

The purpose of the present study was to understand the nature of surface of nc-*Ni* that forms a passive film in 1M H_2SO_4 , using electrochemical impedance spectroscopy (EIS) technique. Rather than looking at conditions immediately on immersion, the study was focused on corrosion behaviour after stabilisation of the free corrosion potential. The nc-*Ni* was produced by pulse electrodeposition using Watt's baths containing two different grain refining agents, as it is known that different grain refining agents produce fine grained deposits in electroplating⁸⁻¹¹. The basic aim was to understand how the surfaces of nc-*Ni* behave when compared with bulk *Ni* on prolonged exposure to a corrosive environment.

2. EXPERIMENTAL PROCEDURES

The nc-*Ni* deposits were obtained on copper substrate by pulse electrodeposition. Copper is the most commonly used substrate for studies on nickel plating, primarily due to structural compatibility between copper and nickel leading to better adhesion of electrodeposits. Copper strips (17 mm x 60 mm x 1 mm) were polished using grades 0/0, 2/0, 3/0, 4/0 emery papers and finally degreased with acetone before the electrodeposition experiments. The plated area was of the size 25 mm x 17 mm. Different anodes of pure nickel, titanium and *Pb-Sn* alloy were initially tried for the electrodeposition². The *Pb-7 wt per cent Sn* alloy was found to be most suitable anode, as it was insoluble and could be reused for several experiments. Plating was performed only on the surface facing the anode. The other surface was coated with enamel to render it electrically insulating. Pulse electrodeposition was performed with a potentiostat (model 263A, Princeton Applied Research (PAR), USA).

The parameters used in the pulsing experiments were $t_{on} = 5$ ms and $t_{off} = 20$ ms, as per the procedure adopted earlier by Mishra and Balasubramaniam⁵. The total time for each experiment was 150 min with cumulative deposition time of 30 min. The bath was maintained at $45 \text{ }^\circ\text{C} \pm 0.01 \text{ }^\circ\text{C}$ using a constant temperature bath (Julabo F-32, Germany) along with continuous stirring during electrodeposition to avoid concentration gradients. Each electrodeposition experiment was performed with a fresh bath. The bath compositions were: nickel sulphate ($NiSO_4 \cdot 6H_2O$)-

240 gm/l, nickel chloride ($NiCl_2 \cdot 6H_2O$)-30 gm/l, and boric acid (H_3BO_3)-30 gm/l. Two different grain refining agents were used separately in the bath: sodium citrate 25 gm/l in one bath and saccharin 10 gm/l in the other.

The x-ray diffraction (XRD) patterns were obtained from the electrodeposited surfaces in a Rich Seifert 2000D diffractometer using $Cu K_\alpha$ radiation. Instrumental broadening was calculated using a standard annealed microcrystalline nickel sample of grain size 61 μm . The grain size was determined using Scherer equation and the procedure is described elsewhere⁵.

Electrochemical testing of bulk nickel, copper (substrate) and electrodeposited nickel was performed in order to compare with the electrochemical behaviour of nc-*Ni* coatings. Electrochemical studies on bulk *Ni* were performed in a round bottom electrochemical polarization cell. The bulk *Ni* sample was mounted in epoxy after providing electrical connection in the backside. The sample was polished using 1/0, 2/0, 3/0, 4/0 emery papers and cleaned with acetone prior to each test. No mechanical polishing was performed on the electroplated nc-*Ni*. For electrochemical testing of copper and electroplated nickel, a flat cell was used. The electrolyte used in all the experiments was freely-aerated 1M H_2SO_4 . Duplicate experiments were conducted and the results were reproducible.

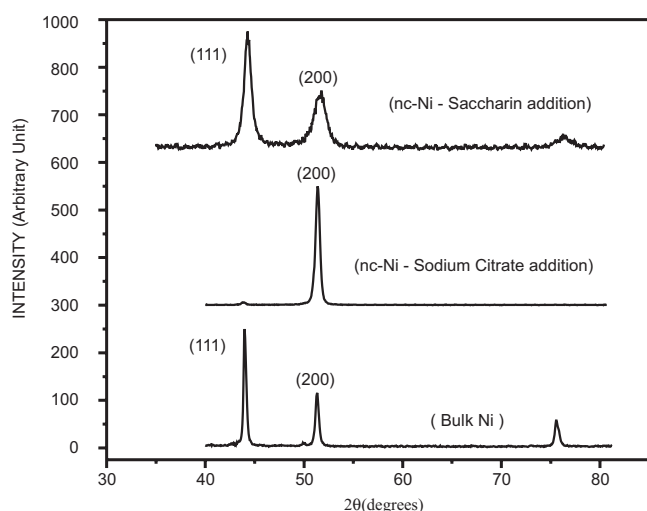
The EIS studies were conducted at free corrosion potential (FCP) after stabilisation of potential. The scan was conducted in the frequency range of 100 kHz to 10 mHz at a sinusoidal voltage amplitude of 10 mV (rms). The EIS data were modelled using ZsimpWin software (PAR, USA).

3. RESULTS AND DISCUSSIONS

The results of the pulse electrodeposition experiments are tabulated in Table 1. The average grain size using sodium citrate as grain refining agent was higher than that obtained using saccharin. The XRD patterns of nc-*Ni* further revealed some interesting details (Fig. 1). Texturing was evident in the electrodeposited nickel using sodium citrate in the bath because $I_{(111)}/I_{(200)}$ [i.e., the relative intensities of (111) and (200) peaks] were found

Table 1. Experimental results for pulse electrodeposition.

Parameter	Exp 1	Exp 2	Exp 3	Exp 4
Grain refiner	Sodium citrate	Sodium citrate	Saccharin	Saccharin
Current density (A/ cm ²)	0.30	0.26	0.26	0.26
Current efficiency (%)	67.20	69.15	77.90	70.02
$I_{(111)}/I_{(200)}$	0.04	0.05	1.95	2.50
Calculated grain size (nm)	27	32	18	16
Thickness of nc-Ni deposits (μm)	124	110	123	111

**Figure 1. XRD patterns obtained from surface of nc-Ni and bulk Ni using Cu K_α radiation.**

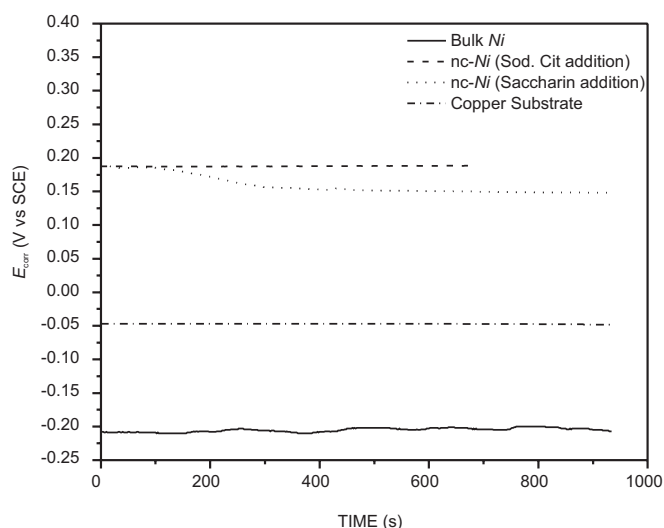
to be 0.04–0.05. This ratio is 2.4 for bulk nickel containing randomly oriented grains. Similar ratios were observed in case of nc-Ni obtained with saccharin addition to the plating bath. These results indicate that there was preferential growth in case of nc-Ni with sodium citrate as additive and the possible role of grain refining agent in causing texturing. It is anticipated that adsorption of sodium citrate on {111} planes would retard the growth of {111} planes, while facilitating the growth of {200} planes.

The variation of free corrosion potential as a function of time for bulk and nc-Ni is shown in Fig. 2. The free corrosion potential for nc-Ni was nobler compared to that for bulk Ni. The free corrosion potentials of nc-Ni produced using two different grain refining agents were similar (Fig. 2). The nobler free corrosion potentials for nc-Ni have been explained based on the change in kinetics for the hydrogen evolution reaction⁵ on nc-Ni.

The EIS was conducted at free corrosion potential at which the material is in condition of active corrosion. The data obtained for nc-Ni and bulk Ni have been compared in Fig. 3 in the form of Nyquist plots. The shape of the curves obtained can be approximated to semicircle, which can be modelled by considering just one time constant. The EIS data obtained was modelled using $R_s(Q_{dl}R_{dl})$ circuit where, R_s is the solution resistance, Q_{dl} is the constant phase element for electrical double layer and R_{dl} is the polarization resistance.

Q_{dl} is a constant phase element comparable to capacitors. Double layer capacitance in electrochemical systems does not behave like an ideal capacitor, but rather there is some amount of leakage current through it. The impedance of a constant phase element is defined as¹².

$$Z = [Q(j\omega)^n]^{-1} \quad (1)$$

**Figure 2. Variation of free corrosion potential as a function of time for bulk Ni, nc-Ni and copper substrate.**

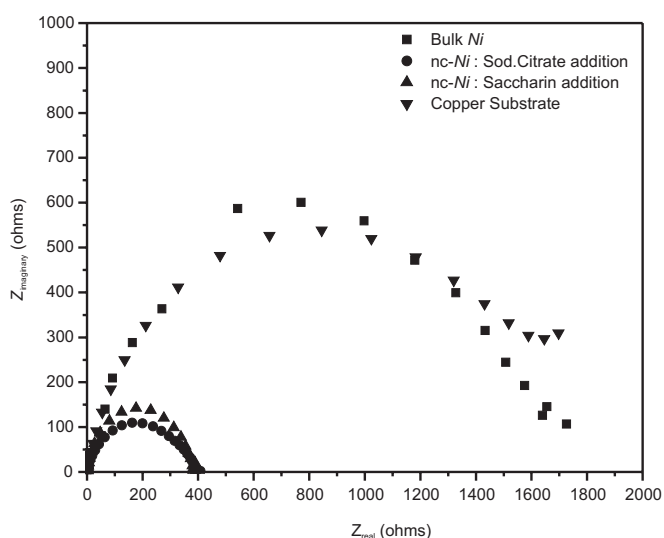


Figure 3. Nyquist plots of EIS data obtained at free corrosion potential for bulk *Ni*, *nc-Ni* and copper substrate.

For a constant phase element, the exponent n is less than one which represents its deviation from ideality ($n=1$).

The parameters obtained by modelling of EIS data are tabulated in Table 2. The solution resistance was almost similar. Q_{dl} for bulk *Ni* sample as well as *nc-Ni* sample was nearly same. Similarly, the n values were comparable and close to 1. This indicates almost capacitive nature of double layer for all the three samples. A higher R_{dl} was obtained for bulk *Ni* compared to *nc-Ni*. This implies that bulk *Ni* was more resistant to anodic dissolution once the free corrosion potential had stabilised. This is an interesting result because it indicates that once free corrosion conditions have been established, the surface of *nc-Ni* is more prone to corrosion than *Ni*.

In order to gain insights on the nature of surface of *nc-Ni*, the surfaces were observed in an atomic

force microscope (AFM) (Fig. 4). The dark regions in the AFM images indicate the valleys, which probably indicate the pores. This has been further confirmed by the porosity measurement using the electrochemical data. The total coating porosity can be evaluated by the following¹³ equation:

$$F = \frac{R_{ps}}{R_{pc}} \times 10^{-|\Delta E_{corr} / \beta_a|} \quad (2)$$

where, F is the total coating porosity, R_{ps} the polarisation resistance of the substrate obtained from EIS data (R_{dl} of copper from Table 2), R_{pc} the polarization resistance of the coated system (Table 2), ΔE_{corr} is the difference of the corrosion potential between the coating and the substrate which is approximately of the order of 0.25 V (Fig. 2). The anodic Tafel slope (β_a) of the substrate was determined by anodic polarization of copper substrate in 1M H_2SO_4 solution and was found to be 40 mV/decade, which is typical of activation controlled anodic polarisation.

According to this, the *nc-Ni* coating on copper substrate possessed 0.00025 per cent porosity with sodium citrate as additive agent and 0.0014 per cent porosity with saccharin as additive. This is comparable to the porosity values reported in the literature using electrochemical data¹³. Thus, the porous nature of the *nc-Ni* deposits could be related to the lower corrosion resistance of *nc-Ni* after stabilisation of free corrosion potential.

4. SUMMARY

The *nc-Ni* deposits were obtained by pulse electrodeposition using Watts's bath using sodium citrate and saccharin as grain refining agents. The grain size was higher for the *nc-Ni* deposited using sodium citrate but, on the contrary, porosity was

Table 2. Parameters obtained by modelling EIS data obtained at free corrosion potential for bulk *Ni* and *nc-Ni*.

	Bulk <i>Ni</i>	<i>nc-Ni</i> (Sodium citrate)	<i>nc-Ni</i> (Saccharin)	Copper (Substrate)
R_s (ohm.cm ²)	0.868	0.444	1.963	2.593
Q_{dl} (? S.s ⁿ .cm ²)	28.90	57.59	52.88	69.22
n_{dl}	0.89	0.82	0.87	0.80
R_{dl} (ohm.cm ²)	1587	361	376	1411

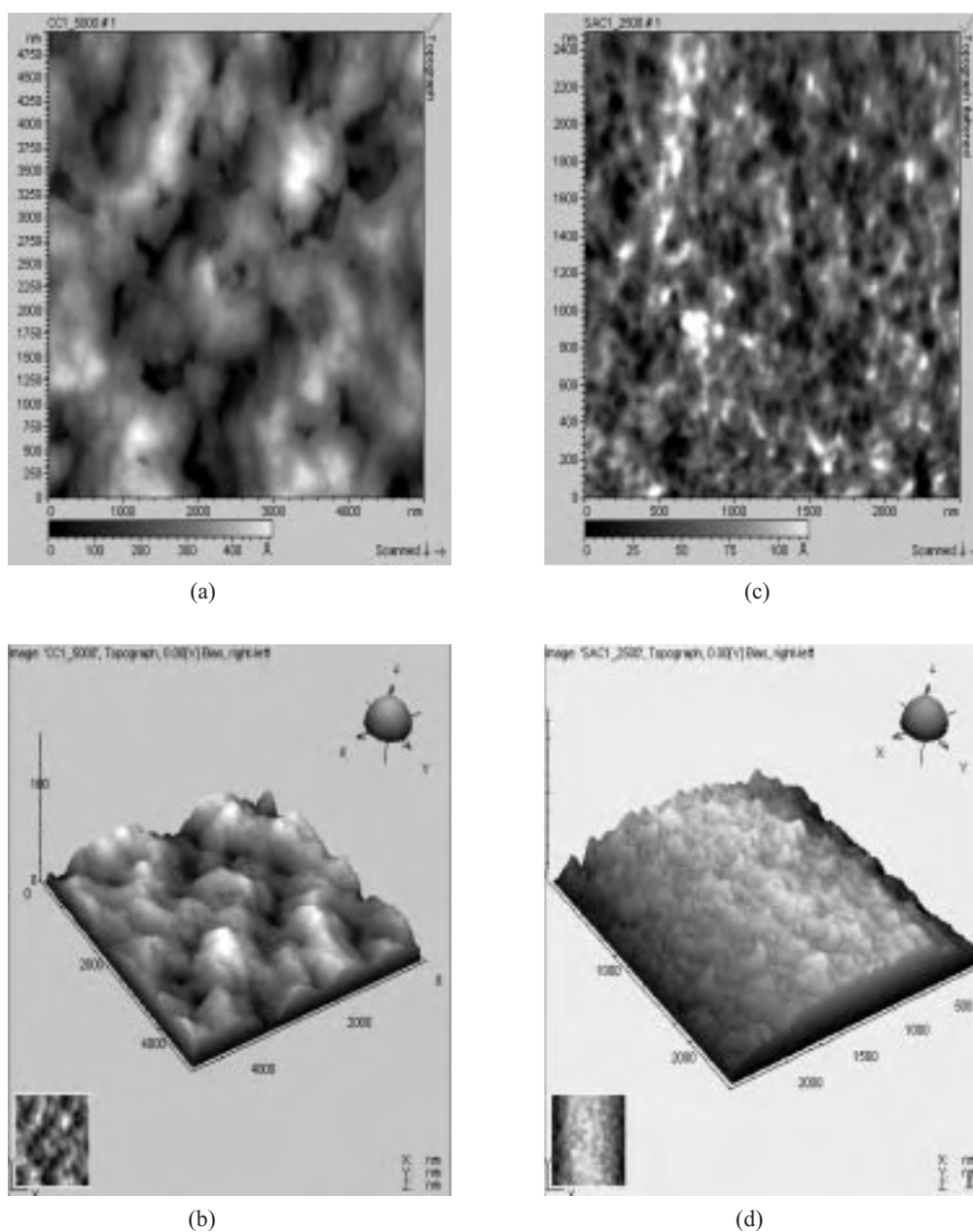


Figure 4. (a) and (c) 2-D AFM images of surface of nc-*Ni* revealing its porous nature for sodium citrate and saccharin additions, respectively, and (b) and (d) 3-D AFM images of surface of nc-*Ni* revealing its porous nature for sodium citrate and saccharin additions, respectively.

found to be approximately an order lower than that with saccharin addition. Texturing was observed in case of nc-*Ni* obtained with sodium citrate as additive. The nature of surfaces of nc-*Ni* was compared with that of bulk *Ni* by electrochemical impedance spectroscopy studies in 1M H_2SO_4 after stabilisation at free corrosion potential. Polarisation resistance for nc-*Ni* was lower compared to that

of bulk *Ni*. The porous nature of nc-*Ni* deposits has been related their lower resistance.

REFERENCES

1. Zimmerman, A.F.; Clark, D.G.; Aust, K.T. & Erb, U. Pulse electrodeposition of *Ni-SiC* nanocomposite. *Materials Letters*, 2002, **52**, 85-90.

2. Mishra, R. Studies on nanocrystalline nickel synthesised by electrodeposition. Department of Materials and Metallurgical Engineering, Indian Institute of Technology, Kanpur, India. MTech Thesis.
3. Mishra, R.; Basu, B. & Balasubramaniam, R. Effect of grain size on the tribological behavior of nanocrystalline nickel. *Mat. Sci. Engg. A*, 2004, **373**, 370-73.
4. Rofagha, R.; Langer, R.; El-Sherik, A.M.; Palumbo, G. & Aust, K.T. The corrosion behaviour of nanocrystalline nickel. *Scripta Materials*, 1991, **25**, 2867-872.
5. Mishra, R. & Balasubramaniam, R. Effect of nanocrystalline grain size on the electrochemical and corrosion behaviour of nickel. *Corrosion Science*, 2004, **46**, 3019-029.
6. Kim, S.H.; Aust, K.T.; Erb, U.; Gonzalez, F. & Palumbo, G. A comparison of the corrosion behaviour of polycrystalline and nanocrystalline cobalt, *Scripta Materials*, 2003, **48**, 1379-384.
7. Zeiger, W.; Schneider, M.; Scharnwber, D. & Worch, H. Corrosion behaviour of nanocrystalline FeAl8 alloy. *Nanostructural Materials*, 1995, **6**, 1013-016.
8. Natter, H.; Schmelzer, M. & Hempelmann, R. Nanocrystalline nickel and nickel-copper-alloys- Synthesis, characterization and thermal stability. *J. Mater. Res.*, 1998, **13**, 1186-197.
9. Youssef, Kh.M.S.; Koch, C.C. & Fedkiw, P.S. Improved corrosion behaviour of nanocrystalline zinc produced by pulse-current electrodeposition. *Corrosion Science*, 2004, **46**, 51-64.
10. Rofagha.; Splinter, S.J.; Erb, U. & McIntyre, N.S. XPS characterization of the passive films formed on nanocrystalline nickel in sulphuric acid. *Nanostructural Materials*, 1994, **4**, 69-78.
11. Afshar, A.; Dolati, A.G. & Ghorbani, M. Electrochemical characterization of the Ni-Fe alloy electrodeposition from chloride-citrate-glycolic acid solutions. *Mat. Chem. Phys.*, 2003, **77**(2), 352-58.
12. Electrochemical Impedance Spectroscopy: A primer.
http://www.gamry.com/App_Notes/EIS_Primer/EIS_Primer.htm
13. Ahn, S.H.; Lee, J.H.; Kim, H.G. & Kim, J.G. A study on the quantitative determination of through-coating porosity in PVD-grown coatings. *Appl. Surf. Sci.*, 2004, **233**, 105-14.